Radiative quantum efficiency in an InAs/AlSb intersubband transition

Clement Faugeras, Aaron Wade, Aude Leuliet, Angela Vasanelli, Carlo Sirtori, Georgy Fedorov, Dmitry Smirnov, Roland Teissier, Alexei Baranov, David Barat, et al.

Radiative quantum efficiency in an InAs/AlSb intersubband transition

C. Faugeras,[1] A. Wade,[2] A. Leuliet,[1,3] A. Vasanelli,[1] C. Sirtori,[1,*] G. Fedorov,[2]
D. Smirnov,[2] R. Teissier,[4] A.N. Baranov,[4] D. Barate,[4] and J. Devenson[4]

[1] *Matériaux et Phénomènes Quantiques, Université Paris 7, 75251 Paris Cedex 05, France*
[2] *National High Magnetic Field Laboratory 1800 E. Paul Dirac Dr. Tallahassee, FL 32310-3706*
[3] *Thales Research and Technology, Route departementale 128, 91767 Palaiseau cedex, France*
[4] *Centre dElectronique et de Micro-optoélectronique de Montpellier, UMR 5507 CNRS - Université Montpellier II, 34095 Montpellier Cedex 05, France*

(Dated: July 25, 2006)

The quantum efficiency of an electroluminescent intersubband emitter based on InAs/AlSb has been measured as a function of the magnetic field up to 20T. Two series of oscillations periodic in 1/B are observed, corresponding to the elastic and inelastic scattering of electrons of the upper state of the radiative transitions. Experimental results are accurately reproduced by a calculation of the excited state lifetime as a function of the applied magnetic field. The interpretation of these data gives an exact measure of the relative weight of the scattering mechanisms and allows the extraction of material parameters such as the energy dependent electron effective mass and the optical phonon energy.

PACS numbers: 63.22.+m, 78.60.Fi, 85.60.Bt

The very short subband lifetime, generally in the order of 1ps, is one of the major limitation to the optical gain of mid-infrared (MIR) quantum cascade (QC) lasers[1]. These unipolar devices are the only semiconductor lasers operating in continuous wave up to room temperature[2,3] in the 4 - 12μm wavelength range and have a great potential for future applications involving molecular spectroscopy. The understanding of the fundamental limits controlling the upper state lifetime will be very beneficial for the ultimate design of these quantum devices.

It is generally assumed that the short lifetime of electrons on excited subbands is totally controlled by the interaction of electrons with optical phonons. However, this scattering mechanism is not the only factor which contributes to the lifetime. Indeed, it has been recently demonstrated that other well known fundamental elastic diffusive phenomena such as interface roughness and alloy disorder can have scattering times of the same order of that induced by the electron-phonon interaction[4], thus clearly contributing to the final lifetime of electrons on excited subbands. These studies have been conducted by applying a strong magnetic field parallel to the growth axis, which breaks the in-plane free particle-like dispersion and reduces the dimensionality of the carrier motion. By tuning the magnetic field intensity it is possible to control the excited state lifetime of an intersubband transition by inhibiting or enhancing the elastic and inelastic scattering resonances. This leads to oscillations of the excited state lifetime and, as a consequence, of both the light intensity and the electrical characteristics of the device[5,6,7].

Previous works have been concentrating on MIR QC lasers. The optical power oscillations as a function of the magnetic field, P(B), reveal the presence of both the inelastic and the elastic scattering of carriers[4]. Because these oscillations are quasi-periodic in 1/B, an electron scattering spectroscopy becomes possible by performing a Fourrier analysis of P(1/B), which provides the characteristic energies involved in the scattering mechanisms. Until today the electron scattering spectroscopy in high magnetic fields has been performed on QC lasers only. In the context of a laser structure the information that can be extracted are related to the variation of the population inversion, therefore to the difference between the lifetime of the upper state and that of the lower state of the laser transition, $\tau_2 - \tau_1$. To get direct information solely on the lifetime of electrons on excited subbands one should examine an electroluminescent structure. In this case the light intensity is directly proportional to the population of electrons on the upper state of the radiative transition, thus to its lifetime.

In this article, we present a scattering spectroscopy investigation of a two-level electroluminescent structure specially designed to obtain information about the fundamental mechanisms that control the lifetime of an excited subband in the InAs/AlSb material system. This material system has recently been exploited to produce lasers in the 3-5μm wavelength range of energy with room temperature laser emission[8], inter-subband emission with a wavelength down to 2.5μm has also been reported[9]. Moreover, this heterostructure is composed by binary materials only and therefore the alloy scattering cannot contribute to the upper state lifetime. Our experiment shows also that it is possible to perform scattering spectroscopy on weak electroluminescence signal from a MIR QC structure.

Fig. 1 shows the conduction band diagram of the two-level InAs/AlSb active region for an applied electric field of 22 kV/cm. It is composed of an injector miniband injecting electrons into the second level of a quantum well (state labelled 2 in Fig. 1). Electrons can then be scattered on the first subband of this quantum well (state labelled 1 in Fig. 1) either in a radiative way, or by

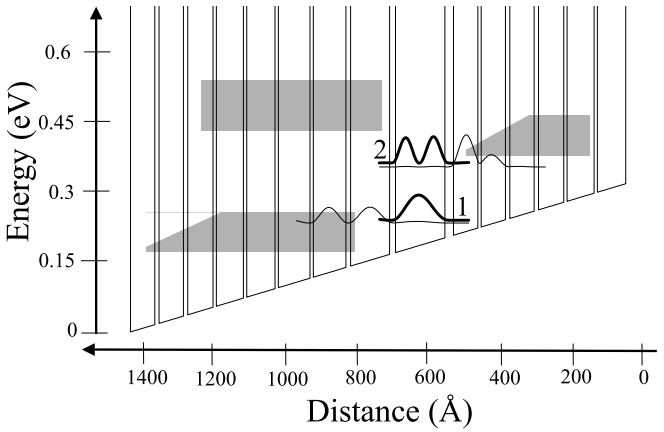

FIG. 1: Conduction band diagram of one period of the active region of the two levels quantum cascade structure. The radiative transition involves the first two levels in the central quantum well (thick solid lines labelled 1 and 2). The gray blocks indicate some of the superlattice minibands. From the injection barrier, the layer sequence in angstroms is (bold layers are AlSb, roman layer are InAs, doped layers are underlined): **24**/132/**16**/104/**14**/90/**10**/84/**10**/76/**10**/72/**10**/68/**12** /65/**12**/65/**10**/65.

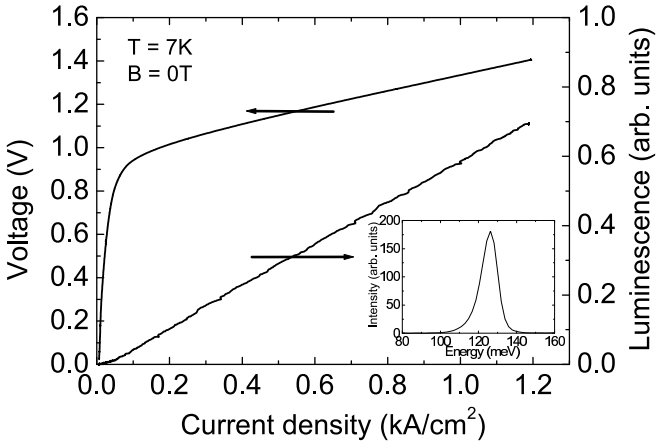

FIG. 2: Voltage and electroluminescence intensity as a function of the injected current density in pulsed operation (77 μs at 3.11 kHz) in a 80 × 80 μm^2 square mesa at T = 7K. Inset: Emission spectrum measured at 77 K.

elastic or inelastic scattering. The active region is composed of 10 periods in series. For electrical and optical characterization, non-alloyed Cr-Au contacts were evaporated and the samples were processed into square mesas of $80\mu m \times 80\mu m$. The substrate has been polished at an angle of 45° with respect to the growth axis to collect the luminescence. Measurements have been performed in pulsed operation with pulses of 70 μs at a repetition rate of 3.11 kHz.

The electrical and optical characteristics of this structure are summarized in Fig. 2 which shows the evolution of the voltage and of the electroluminescence measured with a blocked impurity band (BIB) detector as a function of the injected current density at a temperature of 7K and at $B = 0T$. For voltages higher than 1 V, the different periods of the structure are aligned and thus electrons can tunnel from the injector into the excited state of the quantum well. The luminescence shows a well defined linear dependance with the injected current, showing that the quantum efficiency, at a fixed temperature, is constant with the injected current. As can be seen in the inset of Fig. 2, the emission spectrum measured with a Nicolet Fourier Transform Spectrometer is centered at 126 meV with a full width at half maximum of 10 meV.

The experiment we have performed consists of fixing the voltage at a constant value above the alignment voltage and then measuring the evolution of the injected current and the luminescence intensity as a function of the magnetic field applied parallel to the growth axis. The results of this experiment for a constant voltage of V = 1.44 V are presented in Fig. 3 for magnetic fields up to 22 T. With increasing magnetic fields, two effects are observed. The first effect is a strong decrease of the injected current and as a consequence, of the light intensity. The second effect is a series of oscillations in the injected current and the luminescence intensity superimposed to the decreasing background.

The strong decrease of the current as a function of the external magnetic field is probably due to the magneto resistance that appears in the two contacts and that reduces the voltage applied to the active region of the order of 25% between $B = 0T$ and $B = 20T$. For our QCS, the energy of the transition doesn't change within 1% of this variation of the voltage and only the injection efficiency is affected. We have performed experiments on similar two-level QCS but elaborated in other material systems that showed the same behavior. For values of the magnetic field above 20T, the current injected into the structure becomes smaller than 5 mA and the luminescence signal can no longer be detected.

The oscillations observed in both current and luminescence intensity as a function of the magnetic field can be extracted from the raw data by substracting a smoothed background. The oscillatory components of both the current and the luminescence are presented in the lower panel of Fig. 4. These oscillations are interpreted as revealing the magnetic field modulation of the excited state lifetime. They are in anti-phase and can be explained as follows: When a Landau level of the fundamental state $|1, N\rangle$ (where 1 refers to the electronic subband and N is the Landau level index), is in resonance with the first Landau level of the excited state $|2, 0\rangle$, electrons can be elastically scattered into the state $|1, N\rangle$ which has no oscillator strength with $|1, 0\rangle$. Therefore, the electroluminescence decreases. On the contrary, the current increases since the number of available states for the tunnelling has strongly increased. In fact, electrons can tunnel not only from the injector into $|2, 0\rangle$ but also into $|1, N\rangle$. When the magnetic field is such

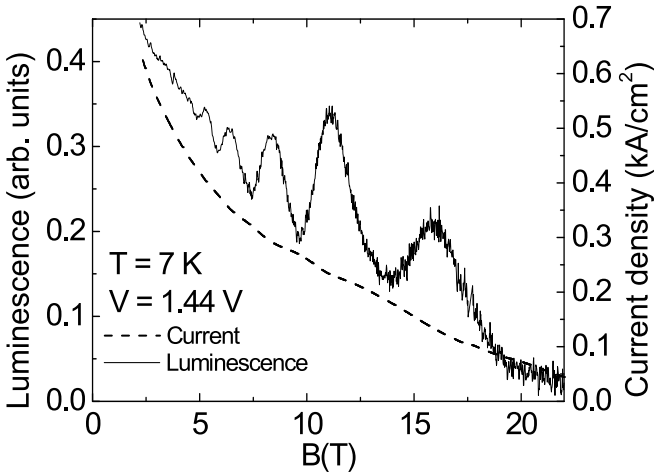

FIG. 3: Evolution of the injected current (dashed line) and of the luminescence (solid line) as a function of the magnetic field at a fixed voltage of V = 1.44 V in pulsed operation.

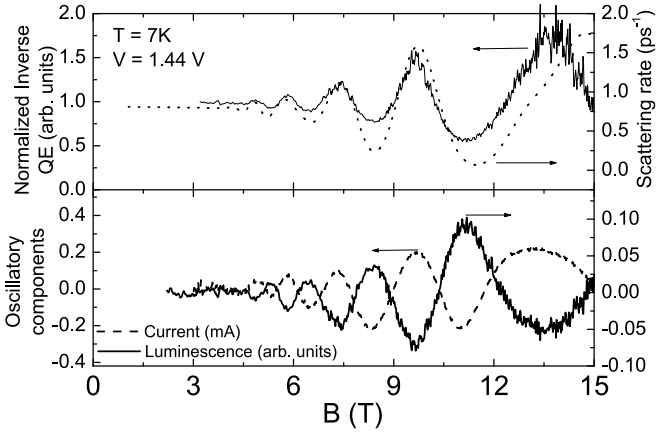

FIG. 4: Upper panel: Evolution of the inverse quantum efficiency (solid line) and of the calculated excited state scattering rate τ_2 (dashed line) as a function of the magnetic field at a fixed voltage of V = 1.44 V. Lower panel: Oscillatory component of the injected current (dashed line) and of the luminescence intensity (solid line) as a function of the magnetic field.

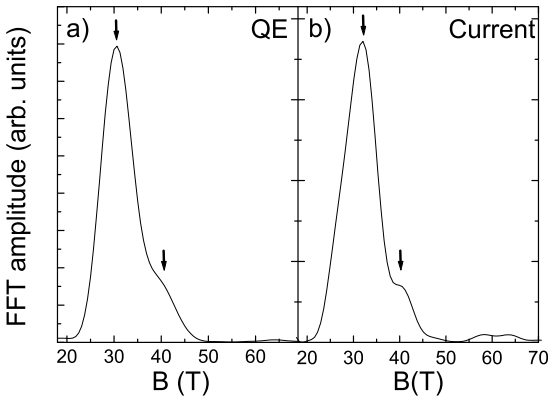

FIG. 5: Fourier transform amplitude in 1/B of a) the quantum efficiency and b) the current. In both cases, two frequencies are extracted $B_{F1} = 30T$ and $B_{F2} = 40T$.

that a Landau level $|1, N\rangle$ of the fundamental state of the quantum well is one LO phonon energy below the first Landau level of the excited state $|2, 0\rangle$, electrons in the excited state can emit resonantly LO phonons and are efficiently scattered. This intersubband-magneto-phonon effect, first observed in double barrier resonant tunnelling diodes[10] and then in QCLs[6], leads to a decrease of the luminescence caused by a decrease of the excited state lifetime in resonant condition. Resonant magnetic fields verify the relation:

$$E_2 - E_1 - p\hbar\omega_{LO} = N\hbar\frac{eB}{m^*(E')} \qquad (1)$$

where $E_2 - E_1$ is the intersubband energy separation which can be measured, $\hbar\omega_{LO}$ is the LO phonon energy, B is the magnetic field, $m^*(E)$ is the energy dependent electron effective mass, N is an integer, $p = 0$ or 1 for the elastic and inelastic series respectively and $E' = E_2 - p\hbar\omega_{LO}$. We recall that these oscillations directly reveal the different electron scattering mechanisms, whereas in QC lasers, the observed oscillations reveal variations in the population inversion ruling laser action.

In order to avoid any artifacts coming from the variations of the current injection with magnetic field, we have determined the quantum efficiency (QE) of our electroluminescent structure by dividing the luminescence signal by the injected current. The evolution of the inverse quantum efficiency as a function of the magnetic field is presented in the upper panel of Fig. 4 (solid line). At $B = 0T$, this quantity is constant as a function of the current as is shown by the linear behavior of the luminescence in Fig. 2. When a magnetic field is applied, the quantum efficiency oscillates with B. A Fourier analysis of these oscillations expressed in inverse magnetic field is presented in Fig. 5 a). Two distinct series are evident, a well defined series with a fundamental field of $B_{F1} = 30T$ and a second series with a lower intensity and with a fundamental field $B_{F2} = 40T$. A similar Fourier analysis of the oscillations of the current is presented in Fig. 5 b) and shows exactly the same characteristic frequencies. These two peaks reveal both the LO phonon inelastic scattering mechanism for the low field series and the elastic scattering for the high field series.

In a simple rate equation model considering a reservoir state injecting electrons with an efficiency η in the excited state 2, the quantum efficiency of a period is defined by:

$$QE = \frac{P}{J} \approx \frac{\eta}{q}\frac{\tau_2}{\tau_{rad}} \qquad (2)$$

where P is the optical power, J the current density, q the electrical charge, η is the injection efficiency, τ_{rad} is the radiative lifetime from level 2 to level 1 (constant with B), τ_2 is the excited state lifetime given by

$\tau_2^{-1} = (\tau_2^{elastic})^{-1} + (\tau_2^{LO})^{-1}$ where $\tau_2^{elastic}$ is the elastic scattering time and τ_2^{LO} is the LO phonon scattering time.

Because it is the quantity that we calculate directly, we present in the upper panel of Fig. 4 the evolution of the calculated excited state scattering rate for our structure (black dashed line) compared to the measured inverse quantum efficiency (black solid line). Experimental results are well reproduced by a calculation considering electron-LO phonon scattering and interface roughness scattering. This calculation is presented in details in Ref.[4] for quantum cascade lasers.

We have been able to reproduce the observed oscillations with a phonon energy of 30.4 meV, in good agreement with values reported in the literature[12]. We have used a Landau level broadening of 6 meV and an energy dependent effective mass taking non-parabolicity into account through a 3 band $\mathbf{k}\cdot\mathbf{p}$ model. The parameters used in the 3 band $\mathbf{k}\cdot\mathbf{p}$ calculation are a band gap of 0.417 eV, a split-off band energy of 0.390 eV and a conduction band effective mass at Γ of $m^* = 0.023m_0$ where m_0 is the electron mass in vacuum. At $B = 0T$, the effective mass of the excited state deduced from our calculation is $0.035m_0$. At low temperatures, the main contribution to the elastic series is the interface roughness scattering[4]. For our calculation, we have used a gaussian autocorrelation of the interface roughness with a correlation length of $60\mathring{A}$ and an average height of the roughness of $2.0\mathring{A}$, slightly lower than values reported so far for this material system[13]. The interface roughness in this material system is of the same amount as the one found in GaAs/AlGaAs interfaces[4]. The deduced scattering times at $B = 0T$ are $\tau_{LO} = 1.57ps$ for the optical phonon scattering and $\tau_{IR} = 6.78ps$ for the interface roughness scattering. For magnetic fields above 15 T, we observe discrepancies between experimental results and the calculation which we think are a consequence of the decrease of the voltage applied to the structure with increasing magnetic fields.

In conclusion, we have reported on the first direct measure of the magnetic field dependence of the quantum efficiency of a two-level QCS up to 20 T. This quantum efficiency oscillates as a function of the magnetic field. Two distinct series of oscillations are identified: the inelastic LO phonon scattering mechanism and, of much smaller intensity, the elastic scattering due to the interface roughness. Experimental data are well reproduced by a calculation of the excited state lifetime considering electron-LO phonon and interface roughness scattering processes. Two-level QCS offers an ideal system to study the electron scattering mechanisms in QCS and to determine their relative importance in QCS of different material systems.

Acknowledgments

We gratefully acknowledge support from EU FP6 Grant STRP 505642 "ANSWER", from EU MRTN-CT-2004-51240 "POISE" and from NHMFL In House Research Program (project 5053).

* Electronic address: carlo.sirtori@paris7.jussieu.fr

[1] J. Faist, F. Capasso, D.L. Sivco, C. Sirtori, A.L. Hutchinson and A.Y. Cho, Science, **264**, 553 (1994).
[2] M. Beck, D. Hofstetter, T. Aellen, J. Faist, U. Oesterle, M. Ilegems, E. Gini and H. Melchior, Science, **295**, 301 (2002).
[3] C. Faugeras, S. Forget, E. Boer-Duchemin, H. Page, J-Y. Bengloan, O. Parillaud, M. Calligaro, C. Sirtori, M. Giovannini and J. Faist, IEEE J. of Quantum Elec., **41**, 1430 (2005).
[4] A. Leuliet, A. Vasanelli, A. Wade, G. Fedorov, D. Smirnov, G. Bastard and C. Sirtori, Phys. Rev. B, **73**, 085311 (2005)
[5] D. Smirnov, C. Becker, O. Drachenko, V.V. Rylkov, H. Page, J. Leotin and C. Sirtori, Phys. Rev. B, **66**, 121305(R) (2002)
[6] D. Smirnov, O. Drachenko, J. Leotin, H. Page, C. Becker, C. Sirtori, V. Apalkov and T. Chakraborty, Phys. Rev. B., **66**, 125317 (2002)
[7] C. Becker, C. Sirtori, O. Drachenko, V.V. Rylkov, D. Smirnov and J. Leotin, Appl. Phys. Lett., **81**, 2941 (2002)
[8] R. Teissier, D. Barate, A. Vicet, C. Alibert, A.N. Baranov, X. Marcadet, C. Renard, M. Garcia, C. Sirtori, D. Revin and J. Cockburn, Appl. Phys. Lett., **85**, 167 (2004)
[9] D. Barate, R. Teissier, Y. Wang and A.N. Baranov, **87**, 051103 (2005).
[10] L. Eaves and G.A. Toombs and F.W. Sheard and C.A. Payling and M.L. Leadbeater and E.S. Alves and T.J. Foster and P.E Simmonds and M. Henini and O.H. Hughes and J.C. Portal and G. Hill and M.A. Pate, Appl. Phys. Lett., **52**, 212 (1988)
[11] C. Sirtori, F. Capasso, J. Faist and S. Scandolo, Phys. Rev. B, **50**, 8663 (1994)
[12] J. Groenen, R. Carles, G. Landa, C. Guerret-Piecourt, C. Fontaine, M. Gendry, Phys. Rev. B, **58**, 10452 (1998)
[13] C.R. Bolognesi and H. Kroemer and J.H. English, Appl. Phys. Lett., **61**, 213 (1992)